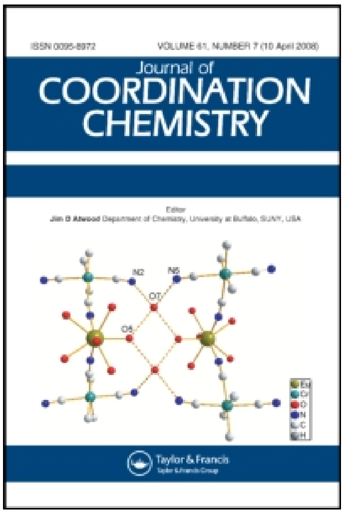

Journal of Coordination Chemistry

Publication details, including instructions for authors and subscription information:
http://www.informaworld.com/smpp/title~content=t713455674

Structural diversity in copper(II) complexes of bis(thiosemicarbazone) and bis(semicarbazone) ligands

H. S. Seleem[a]; B. A. El-Shetary[a]; S. M. E. Khalil[a]; M. Mostafa[a]; M. Shebl[a]
[a] Department of Chemistry, Faculty of Education, Ain Shams University, Roxy, Cairo, Egypt

To cite this Article Seleem, H. S. , El-Shetary, B. A. , Khalil, S. M. E. , Mostafa, M. and Shebl, M.(2005) 'Structural diversity in copper(II) complexes of bis(thiosemicarbazone) and bis(semicarbazone) ligands', Journal of Coordination Chemistry, 58: 6, 479 — 493

To link to this Article: DOI: 10.1080/00958970512331334269

URL: http://dx.doi.org/10.1080/00958970512331334269

Journal of Coordination Chemistry
Vol. 58, No. 6, 15 April 2005, 479–493

Structural diversity in copper(II) complexes of bis(thiosemicarbazone) and bis(semicarbazone) ligands

H. S. SELEEM*, B. A. EL-SHETARY, S. M. E. KHALIL,
M. MOSTAFA and M. SHEBL

Department of Chemistry, Faculty of Education,
Ain Shams University, Roxy, Cairo, Egypt

(*Received 3 May 2004; in final form 19 November 2004*)

Two symmetrical bis(carbazone) ligands, H_4L^1 and H_4L^2, were prepared by condensation of 4,6-diacetylresorcinol with thiosemicarbazide and semicarbazide, respectively. Their structures were elucidated by elemental analyses and IR, electronic and ^{1}H NMR spectroscopy. Both ligands are tetrabasic and contain two sets of SNO (H_4L^1) or ONO (H_4L^2) coordinating sites. Binuclear, trinuclear and dimeric Cu^{II} complexes and also adducts with organic bases were prepared. Reactions of H_4L^1 with several Cu^{II} salts, including Cl^-, AcO^-, SO_4^{2-}, NO_3^- and ClO_4^-, in addition to Cu^I as CuI, afforded different binuclear complexes depending on the salt and the working conditions, except for $CuCl_2$, where a trinuclear complex with a unique mode of bonding was obtained. These complexes reflect the strong coordinating power of Cl^-, SO_4^{2-} and AcO^- compared to ClO_4^-. The mode of bonding and the basicity of the H_4L^1 ligand are also influenced by the counteranion, the pH of the reaction medium, the working conditions and the oxidation state of copper. The reactivity of the binuclear Cu^{II} complexes of both H_4L^1 and H_4L^2 towards 1,10-phenanthroline (Phen), 2,2′-bipyridyl (Bpy), *N*,*N*,*N*′,*N*′-tetramethylethylenediamine (Tmen) and 8-hydroxyquinoline (Oxine; Ox) were investigated. Adducts with organic bases were obtained in the mole ratio 2 : 1 : 1 for H_4L^1 and 2 : 1 : 2 for H_4L^2 [Cu^{II} : ligand : base (base = Phen, Bpy or Ox)], which reflects the difference in size of S and O. With Tmen, dimeric complexes were obtained containing no Tmen molecules instead of the expected adducts for both H_4L^1 and H_4L^2. Evidently the presence of Tmen in the reaction mixture enhances the dimerization process. Characterization and structure elucidation of the complexes was achieved by elemental and thermal analyses, electronic, IR, mass and ESR spectroscopy, as well as conductance and magnetic susceptibility measurements. Finally, the antifungal and antibacterial activities of H_4L^1 and its metal complexes were investigated.

Keywords: Binuclear, trinuclear and dimeric Cu^{II} complexes; Bis(thiosemicarbazone); Bis(semicarbazone)

1. Introduction

Thiosemicarbazones and their metal complexes are of interest [1–3] because of their potentially beneficial pharmacological properties [4,5] and wide variety of bonding

---

*Corresponding author. Email: hsseleem@yahoo.com

Journal of Coordination Chemistry
ISSN 0095-8972 print: ISSN 1029-0389 online © 2005 Taylor & Francis Group Ltd
DOI: 10.1080/00958970512331334269

and stereochemistry [6,7]. They have also been used for the analysis of metals [8], and for device application in telecommunications, optical computing, optical storage and optical information processing [9]. Semicarbazones are among the most important nitrogen–oxygen donor ligands [10]. Both semicarbazone and thiosemicarbazone ligands are capable of acting as neutral or charged ligand moieties. The present investigation deals with the preparation and characterization of a series of new Cu(II) complexes with some bis(semicarbazones) and bis(thiosemicarbazones), in addition to their adducts with 1,10-phenanthroline (Phen), 2,2′-bipyridyl (Bpy) and 8-hydroxyquinoline (Oxine; Ox). This study is a continuation of our work on hydrazones [11] and thiosemicarbazones [12].

2. Experimental

All chemicals, metal nitrates and solvents were either Aldrich, BDH or Merck products. FT-IR spectra were recorded on a Perkin Elmer 1650 spectrometer (4000–200 cm^{-1}) using KBr pellets. Electronic spectra were recorded at room temperature on a Jasco model V-550 UV/VIS spectrophotometer as nujol mulls and/or solutions in DMF. ^{1}H NMR spectra of the ligands and some complexes, in DMSO-d_6 as solvent, were recorded on a Bruker WP 200 SY spectrometer at room temperature using TMS as internal standard. Mass spectra were recorded at 290°C and 70 eV on a Hewlett-Packard MS-5988 instrument. Molar conductivities of 10^{-3} M solutions of the solid complexes in DMF were measured on a Corning conductivity meter NY 14831 model 441. Magnetic susceptibilities of the complexes were measured by the Gouy method at room temperature using a Johnson Matthey, Alfa Products, Model MKI magnetic susceptibility balance. The effective magnetic moments were calculated from the expression $\mu_{\mathrm{eff}} = 2.828(\chi_{\mathrm{M}}T)^{1/2}$ BM, where χ_{M} is the molar susceptibility corrected using Pascal's constants for the diamagnetism of all atoms in the compounds. Carbon, hydrogen, nitrogen, sulfur and chlorine microanalyses were carried out at the Microanalysis Center, Cairo University, Giza, Cairo, Egypt. TG-DSC measurements were carried out on a Shimadzu-50 instrument. Melting points of the complexes were determined using a Rumo instrument, model 3600, three samples, and a concentrated sulfuric acid bath. Antibacterial and antifungal activities were evaluated at the Microbiological Laboratory, Botany Department, Faculty of Girls, Ain Shams University, Egypt.

2.1. *Preparation of H_4L^1 and H_4L^2 ligands*

A mixture of 4,6-diacetylresorcinol (0.01 mol) and thiosemicarbazide or semicarbazide hydrochloride (0.02 mol) dissolved in a minimal amount of water was refluxed for 4 h to yield H_4L^1 and H_4L^2, respectively. The reaction mixture was cooled and the solid formed was filtered off, washed with water, ethanol and finally ether and crystallized from water to DMF. Analytical and physical data for the ligands are shown in table 1.

2.2. *Preparation of the metal complexes*

The following detailed preparations are given as examples and the other complexes were obtained by similar methods.

2.2.1. Preparation of $[(L^1)Cu_2(H_2O)_2]½EtOH$. An ethanolic solution (40 mL) of $Cu(NO_3)_2 \cdot 2½H_2O$ (1.1 g, 4.7 mmol) was added gradually to a suspension of the ligand (H_4L^1) in ethanol (40 mL) (0.8 g, 2.35 mmol). The mixture was refluxed for 5 h and a brown precipitate formed. The precipitate was filtered, washed with ethanol, diethylether and finally air-dried; yield 0.65 g (53%).

2.3. *Preparation of mixed ligand*

An ethanolic solution (40 mL) of $Cu(NO_3)_2 \cdot 2½H_2O$ was added gradually to a suspension of the ligand (H_4L^1 or H_4L^2) in ethanol (40 mL) in a molar ratio of 2 : 1 (M : L). The mixture was refluxed for 30 min, then an ethanolic solution of Oxine, Phen, Bpy or *N*,*N*,*N*′,*N*′-tetramethylethylenediamine (Tmen) was added to the solution in a molar ratio of 2 : 1 : 2 metal ion : ligand : base. The solution was refluxed for 5 h and the precipitates formed were filtered off, washed with ethanol, then ether and finally air-dried.

3. Results and discussion

Structures of the ligands have been elucidated by elemental analysis, electronic, IR and ^1H NMR spectroscopy. The elemental analyses (table 1) are in good agreement with the proposed formulae. The thiosemicarbazone (H_4L^1) and the semicarbazone (H_4L^2) ligands have the following tautomeric forms:

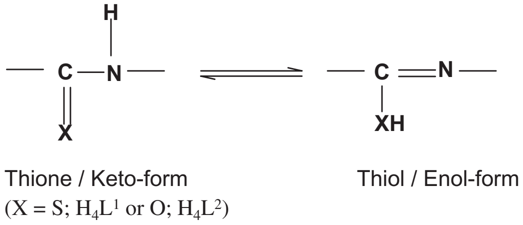

IR spectra of the ligands (table 2) showed broad bands at 2922 and 2885 cm^{-1} assigned to $\nu(OH \cdots N)$ (phenolic group), strong bands at 1618 and 1623 cm^{-1} attributed to $\nu(C{=}N)$ and very strong bands at 3188 and 3206 cm^{-1} assigned to $\nu(NH)$ of H_4L^1 and H_4L^2, respectively. Two strong bands at 3450 and 3405 cm^{-1} and 3350 and 3300 cm^{-1} are assigned to ν_{as} and ν_s of the $–NH_2$ group of H_4L^2 and H_4L^1 ligands, respectively. As both ligands contain the –NHC=X grouping [X = S (H_4L^1) and O (H_4L^2)], they showed the amide group vibrations [13], respectively, at approximately:

(i) 1551 and 1671 cm^{-1} [amide I; $\nu(C{=}S)$ and $\nu(C{=}O)$];
(ii) 1270 and 1274 cm^{-1} [amide II; $\nu(C–N) + \delta(N–H)$];
(iii) 1044 and 1067 cm^{-1} [amide III; $\delta(N–H)$]; and
(iv) 778 and 815 cm^{-1} [amide IV; $\phi(C{=}S)$ and $\phi(C{=}O)$].

These bands support the ketonic nature (thione/keto form) of the ligands in the solid state. The absence of an IR band around 2600 cm^{-1} due to $\nu(SH)$ support the thione nature of the H_4L^1 ligand in the solid state [14]. in addition, the absence of a signal

Table 1. Analytical and physical data for the ligands and their metal complexes.

					Elemental analysis: % found (calc.)				
No.	Reaction	Complex MF [FW]	Color	Yield (%)	C	H	N	S/Cl	M
	H_4L^1	$C_{12}H_{16}N_6O_2S_2$ [340.43]	Pale yellow	77	42.40 (42.34)	4.80 (4.74)	24.35 (24.69)	18.68 (18.84)	–
1	$H_4L^1 + Cu(NO_3)_3 \cdot 2\frac{1}{2}H_2O$	$[(L^1)Cu_2(H_2O)_2]\frac{1}{2}EtOH$ $C_{13}H_{19}N_6O_{4.5}S_2$ Cu_2 [522.55]	Brown	53	29.90 (29.88)	3.70 (3.66)	15.98 (16.08)	12.19 (12.27)	24.00 (24.32)
2	$H_4L^1 + Cu(OAc)_2 \cdot H_2O$	$[(H_2L^1)Cu_2(OAc)_2(H_2O)_3]\frac{1}{2}EtOH$ $C_{17}H_{29}N_6O_{9.5}S_2$ Cu_2 [660.68]	Olive green	64	30.70 (30.91)	4.20 (4.42)	13.00 (12.72)	9.85 (9.71)	19.10 (19.24)
3	$H_4L^1 + CuCl_2$	$[(H_2L^1)_2Cu_3(H_2O)_2Cl_2]EtOH$ $C_{26}H_{38}N_{12}O_7S_4Cl_2Cu_3$ [1020.47]	Olive green	40	30.70 (30.60)	3.70 (3.75)	16.28 (16.47)	12.70/6.76 (12.57)/(6.95)	18.60 (18.68)
4	$H_4L^1 + Cu(ClO_4)_2 \cdot 6H_2O$	$[(HL^1)Cu_2(H_2O)_7]ClO_4$ $(C_{12}H_{27}N_6O_{13}S_2ClCu_2)$ [690.05]	Olive green	38	20.80 (20.89)	3.80 (3.94)	12.33 (12.18)	9.41 (9.29)	18.20 (18.42)
5	$H_4L^1 + CuSO_4 \cdot 5H_2O$	$[(H_2L^1)Cu_2(H_2O)_5SO_4]$ $(C_{12}H_{24}N_6O_{11}S_3Cu_2)$ [651.64]	Green	90	22.10 (22.12)	4.00 (3.71)	12.66 (12.90)	14.89 (14.76)	19.30 (19.50)
6	$H_4L^1 + Cu(NO_3)_2 \cdot 2\frac{1}{2}H_2O$ stirring	$[(HL^1)Cu_2(H_2O)_7]NO_3 \cdot \frac{1}{2}EtOH$ $(C_{13}H_{30}N_7O_{12.5}S_2Cu_2)$ [675.64]	Deep brown	48	22.70 (23.11)	4.40 (4.48)	14.86 (14.51)	9.70 (9.49)	18.70 (18.81)
7	$H_4L^1 + Cu(NO_3)_2 \cdot 2\frac{1}{2}H_2O + LiOH$	$[(H_2L^1)Cu_2(H_2O)_4(NO_3)_2]\frac{1}{2}EtOH$ $(C_{13}H_{25}N_8O_{12.5}S_2Cu_2)$ [684.61]	Deep brown	95	22.50 (22.81)	3.70 (3.68)	16.13 (16.37)	9.70 (9.37)	18.40 (18.56)
8	$H_4L^1 + CuCl_2 + LiOH$	$[(H_2L^1)Cu_2Cl_2(H_2O)_4]EtOH$ $(C_{14}H_{28}N_6O_7Cl_2$ $S_2Cu_2)$ [654.54]	Deep brown	63	25.70 (25.69)	4.30 (4.31)	12.61 (12.84)	9.91/10.68 (9.80)/(10.83)	19.30 (19.42)
9	$H_4L^1 + CuI$	$[(H_4L^1)Cu_2I_2(H_2O)_6] \cdot 1\frac{1}{2}H_2O$ $(C_{12}H_{31}N_6O_{9.5}I_2$ $S_2Cu_2)$ [856.44]	Olive-green	80	16.50 (16.83)	3.10 (3.65)	10.06 (9.81)	7.66 (7.49)	14.60 (14.84)

10	$H_4L^1 + Cu(NO_3)_2 \cdot 2\frac{1}{2}H_2O$ + Ox	$[(H_2L^1)Cu_2(Ox)(H_2O)_5]NO_3 \cdot \frac{1}{2}EtOH$ $(C_{22}H_{33}N_8O_{11.5}S_2Cu_2)$ [784.78]	Olive-green	42	33.50 (33.67)	4.50 (4.24)	14.10 (13.87)	7.60 (7.94)	15.60 (15.73)
11	$H_4L^1 + Cu(NO_3)_2 \cdot 2\frac{1}{2}H_2O$ + Phen	$[(H_2L^1)Cu_2(Phen)(NO_3)(H_2O)_4]NO_3 \cdot 2H_2O$ $(C_{24}H_{34}N_{10}O_{14}S_2Cu_2)$ [877.82]	Olive-green	37	33.00 (32.84)	3.90 (3.90)	15.52 (15.96)	7.60 (7.31)	14.20 (14.48)
12	$H_4L^1 + Cu(NO_3)_2 \cdot 2\frac{1}{2}H_2O$ + Bpy	$[(H_2L^1)Cu_2(Bpy)(NO_3)(H_2O)_4]NO_3 \cdot EtOH$ $(C_{24}H_{36}N_{10}O_{13}S_2Cu_2)$ [863.83]	Olive-green	39	33.40 (33.37)	4.20 (4.20)	15.80 (16.21)	7.80 (7.42)	14.40 (14.71)
13	$H_4L^1 + Cu(NO_3)_2 \cdot 2\frac{1}{2}H_2O$ + Tmen	$[(H_2L^1)_2Cu_2(H_2O)_2]EtOH$ $(C_{26}H_{38}N_{12}O_7S_4Cu_2)$ [886.02]	Green	37	35.40 (35.25)	4.20 (4.32)	18.50 (18.97)	14.72 (14.48)	14.10 (14.34)
	H_4L^2	$C_{12}H_{16}N_6O_4$ [308.30]	Yellowish-orange	75	46.50 (46.75)	5.00 (5.23)	27.01 (27.26)		–
14	$H_4L^2 + Cu(NO_3)_3 \cdot 2\frac{1}{2}H_2O$	$[(HL^2)Cu_2(H_2O)_2]NO_3 \cdot H_2O$ $C_{12}H_{19}N_7O_{10}Cu_2$ [548.42]	Green	54	26.30 (26.26)	3.50 (3.49)	18.10 (17.87)		22.90 (23.16)
15	$H_4L^2 + Cu(NO_3)_2 \cdot 2\frac{1}{2}H_2O$ + Ox	$[(HL^2)Cu_2(H_2O)_2]NO_3 \cdot \frac{1}{4}EtOH$ $C_{12.5}H_{18.5}N_7O_{9.25}Cu_2$ [541.92]	Green	49	27.34 (27.71)	3.66 (3.44)	17.80 (18.09)		23.20 (23.45)
16	$H_4L^2 + Cu(NO_3)_2 \cdot 2\frac{1}{2}H_2O$ + Phen	$[(H_2L^2)Cu_2(Phen)_2(H_2O)_3](NO_3)_2$ $(C_{36}H_{36}N_{12}O_{13}Cu_2)$ [971.85]	Greenish-blue	36	44.46 (44.49)	3.34 (3.73)	17.55 (17.29)		13.00 (13.08)
17	$H_4L^2 + Cu(NO_3)_2 \cdot 2\frac{1}{2}H_2O$ + Bpy	$[(H_2L^2)Cu_2(Bpy)_2(H_2O)_3](NO_3)_2 \cdot H_2O$ $(C_{32}H_{38}N_{12}O_{14}Cu_2)$ [941.82]	Sky-blue	63	40.84 (40.81)	3.65 (4.07)	18.10 (17.85)		13.30 (13.49)
18	$H_4L^2 + Cu(NO_3)_2 \cdot 2\frac{1}{2}H_2O$ + Tmen	$[(H_3L^2)_2Cu_2(H_2O)_4]NO_3 \cdot 2\frac{1}{2}EtOH$ $(C_{25}H_{41}N_{14}O_{18.5}Cu_2)$ [960.78]	Green	47	31.20 (31.25)	4.59 (4.30)	19.96 (20.41)		13.10 (13.23)

Table 2. IR spectral data for H_4L^1 ligand and its metal complexes.

		IR spectral bands (cm^{-1})					
No.	Complex	νOH H_2O/EtOH/phenolic	νC=N free	νC=N coord	νC=S	νC–S	Other bands
	H_4L^1	2922	1618	–	1551	–	
1	$[(L^1)Cu_2(H_2O)_2]\frac{1}{2}EtOH$	3370	1620	1593	–	770	
2	$[(H_2L^1)Cu_2(OAc)_2(H_2O)_3]\frac{1}{2}EtOH$	3500	1622	1593	1539	780	1470; $\nu_{as}(COO^-)$ 1412; $\nu_s(COO^-)$
3	$[(H_2L^1)_2Cu_3(H_2O)_2Cl_2]EtOH$	3390	1620	1594	–	780	303; ν(Cu–Cl)
4	$[(HL^1)Cu_2(H_2O)_7]ClO_4$	3376	1620	1591	–	797	1080; $\nu_3(ClO_4^-)$
5	$[(H_2L^1)Cu_2(H_2O)_5SO_4]$	3381	1621	1590	1533	787	1287, 1087; $\nu_3(SO_4^{2-})$
6	$[(HL^1)Cu_2(H_2O)_7]NO_3 \cdot \frac{1}{2}EtOH$	3397	1622	1592	–	777	1431; $\nu(NO_3^-)$
7	$[(H_2L^1)Cu_2(H_2O)_4(NO_3)_2]\frac{1}{2}EtOH$	3500	–	1591	1533	–	1440 (ν_5); $\nu_{as}(NO_2)$ 1360 (ν_1); $\nu_s(NO_2)$
8	$[(H_2L^1)Cu_2Cl_2(H_2O)_4]EtOH$	3337	–	1594	1533	–	302; ν(Cu–Cl)
9	$[(H_4L^1)Cu_2I_2(H_2O)_6]1\frac{1}{2}H_2O$	3387	–	1600	1535	–	241; ν(Cu–I)
10	$[(H_2L^1)Cu_2(Ox)(H_2O)_5]NO_3 \cdot \frac{1}{2}EtOH$	3500	1623	1596	1538	780	1412; $\nu(NO_3^-)$ 1492; νC=N (Oxine)
11	$[(H_2L^1)Cu_2(Phen)(NO_3)(H_2O)_4]NO_3 \cdot 2H_2O$	3500	1617	1597	1543	779	1410; $\nu(NO_3^-)$ 1491; νC=N (Phen)
12	$[(H_2L^1)Cu_2(Bpy)(NO_3)(H_2O)_4]NO_3 \cdot EtOH$	3373	1620	1597	1537	777	1409; $\nu(NO_3^-)$ 1491; νC=N (Bpy)
13	$[(H_2L^1)_2Cu_2(H_2O)_2]EtOH$	3414	1617	1588	1514	771	
		νOH H_2O/EtOH/phenolic	νC=O	νC=N free	νC=N coord		Other bands
	H_4L^2	2885	1671	1623	–		
14	$[(HL^2)Cu_2(H_2O)_2]NO_3 \cdot H_2O$	3434	1659	1627	1588		1394; $\nu(NO_3^-)$
15	$[(HL^2)Cu_2(H_2O)_2]NO_3 \cdot \frac{1}{4}EtOH$	3460	1652	1625	1586		1391; $\nu(NO_3^-)$
16	$[(H_2L^2)Cu_2(Phen)_2(H_2O)_3](NO_3)_2$	3430	1663	1627	1603		1390; $\nu(NO_3^-)$ 1480; νC=N (Phen)
17	$[(H_2L^2)Cu_2(Bpy)_2(H_2O)_3](NO_3)_2 \cdot H_2O$	3439	1651	1626	1599		1394; $\nu(NO_3^-)$ 1477; νC=N (Bpy)
18	$[(H_3L^2)_2Cu_2(H_2O)_4]NO_3 \cdot 2\frac{1}{2}EtOH$	3387	1675	1625	1597		1398; $\nu(NO_3^-)$

at *ca* 4.0 ppm in the ^{1}H NMR spectra attributable to the SH proton provides further strong evidence of the thione form of H_4L^1 ligand even in the solution state [14].

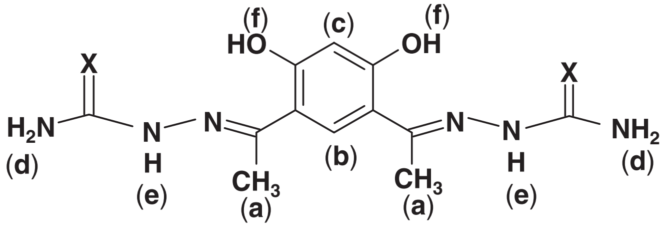

	δ (ppm)					
	H^a	H^b	H^c	H^d	H^e	H^f
H_4L^1 (X = S)	2.35(6H)	6.35(1H)	7.64(1H)	7.98(4H)	10.25(2H)	12.62(2H)
H_4L^2 (X = O)	2.27(6H)	6.27(1H)	7.53(1H)	7.99(4H)	9.57(2H)	11.65(2H)

Scheme 1. ^{1}H NMR spectra of the ligands in DMSO-d_6.

Electronic spectra of the ligands in DMF showed bands in the ranges 225–273, 297–300 and 333–345 nm. The higher energy bands in the region 225–273 nm are assigned to π–π* transitions of the azomethine linkage and the aromatic benzene ring. The medium energy bands in the region 297–300 nm are assigned to *n*–π* transitions of the C=O, C=N and C=S groups. Finally, the lower energy bands in the region 333–345 nm are attributed to charge transfer (CT) transitions within the molecules.

^{1}H NMR spectral data (δ ppm) of the ligands relative to TMS (0 ppm) in DMSO-d_6 lend further support to the suggested structures of the ligands (scheme 1). All peaks were recorded as singlets and are exchangeable with D_2O except the methyl and aromatic protons. These data, together with the data derived from the elemental analysis, IR and electronic spectra, confirmed the structures given for these ligands.

3.1. *The metal complexes*

The ligands H_4L^1 and H_4L^2 are tetrabasic and have two sets of SNO and ONO donor sites; therefore, they could react with all metal ions in the molar ratio 2 : 1 metal : ligand. Elemental analyses (table 1) agreed with the proposed formulas. The bis(thiosemicarbazone) ligand, H_4L^1, was therefore allowed to react with several Cu^{II} salts, e.g. Cl^-, NO_3^-, AcO^-, ClO_4^- and SO_4^{2-}, in addition to Cu^I as CuI, in order to determine the effect of the counterions and the experimental conditions on the products. These reactions afforded binuclear complexes and only one trinuclear complex (**3**) for $CuCl_2$. However, these binuclear and trinuclear complexes reflect the noncoordinating or weakly coordinating power of the ClO_4^- anion as compared to the strongly coordinating power of the Cl^-, SO_4^2 and AcO^- anions (schemes 2–4). For H_4L^2, only Cu^{II} nitrate was tried (scheme 2).

The bis(carbazone) ligands, H_4L^1 and H_4L^2, were also allowed to react with Cu^{II} nitrate in the presence of the bases Phen, Bpy, Tmen and Oxine. These reactions afforded adducts having the molar ratio 2 : 1 : 1 for H_4L^1 and 2 : 1 : 2 for H_4L^2 (scheme 5).

For Tmen, dimeric complexes were obtained instead of the expected adducts (scheme 6; complexes **13** and **18**). Evidently a base-catalyzed dimerization reaction occurs.

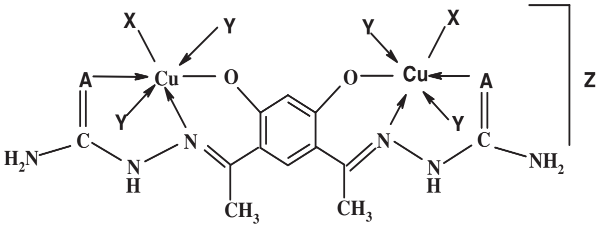

A	X	Y	Z	Complex
S	H_2O	–	–	**1**
S	NO_3^-	H_2O	–	**7**
S	Cl–	H_2O	–	**8**
O	H_2O	–	NO_3^-	**14**,**15** (table 1)

Scheme 2. Proposed structures of Cu^{II} complexes of both H_4L^1 and H_4L^2.

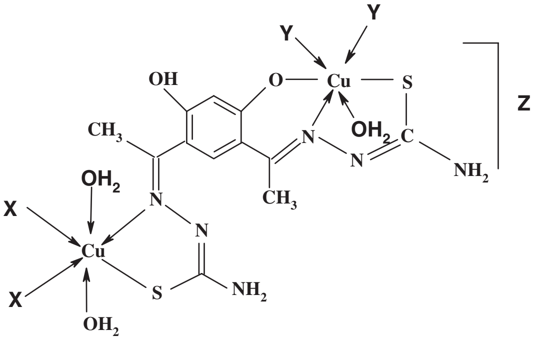

X	Y	Z	Complex
H_2O	H_2O	ClO_4^-	**4**
H_2O	H_2O	NO_3^-	**6**
O,O (bidentate SO_4^{2-})	H_2O	–	**5**
O,O (bidentate AcO^-)		–	**2**

Scheme 3. Proposed strucutres of the binuclear Cu^{II}-complexes of H_4L^1.

The above stereochemical diversity and the various structural possibilities, in addition to the variety of modes of bonding, are attributed to the different tautomeric structures of the ligands H_4L^1 and H_4L^2 and the tendency of both S and O donors to form bridges. All attempts to isolate adducts with OO donors, such as benzil and 2-hydroxyacetophenone, were unsuccessful. Attempts to isolate mononuclear complexes were also unsuccessful.

All of the complexes prepared are stable at room temperature, nonhygroscopic and insoluble in water; their colors range from olive green to dark brown. The melting

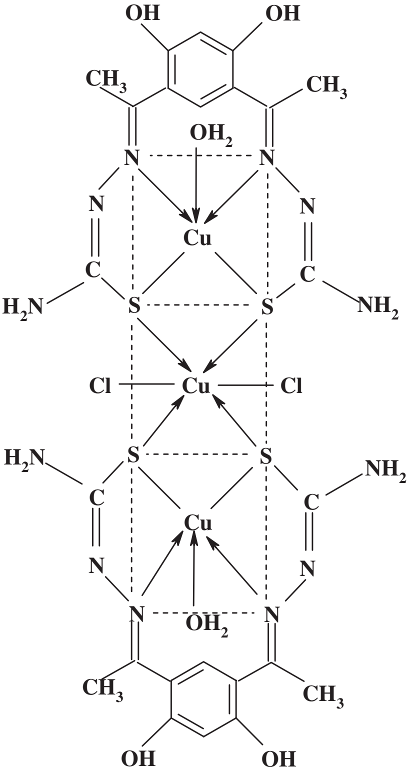

(3)

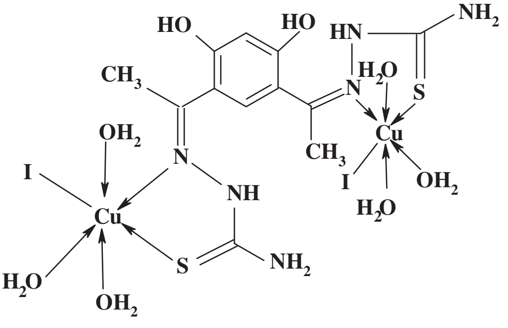

(9)

Scheme 4. Proposed structures of trinuclear Cu^{II} and binuclear Cu^{I} complexes of H_4L^1.

points of all ligands and complexes are above 300°C, except for $[(H_3L^2)_2Cu_2(H_2O)_4](NO_3)_2 \cdot \frac{1}{2}EtOH$ (**18**), which has a melting point of 210°C.

The molar conductance values of around $1 \times 10^{-3}\,mol\,dm^{-3}$ in DMF (table 3) classify the complexes as electrolytes, 1 : 1 (complexes **4**, **6**, **10–12**, **14** and **15**) and 2 : 1 (complexes **16–18**), and nonelectrolytes, that is neutral complexes (the rest). For the 1 : 1 and 2 : 1 electrolytes, the molar conductance values fall in the expected range

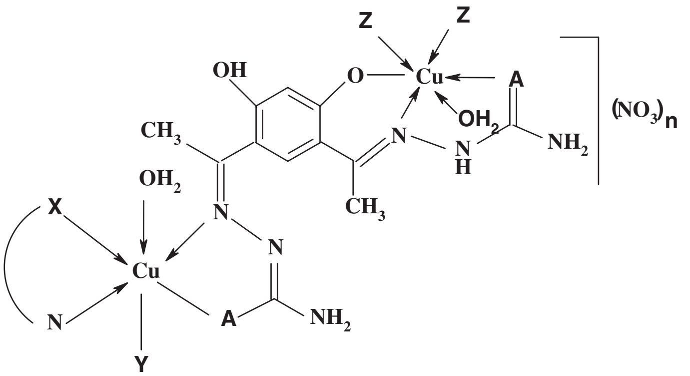

A	X	Y	Z	*n*	Complex
S	O; Ox	H_2O	H_2O	1	**10**
S	N; Phen	NO_3^-	H_2O	1	**11**
S	N; Bpy	NO_3^-	H_2O	1	**12**
O	N; Phen	H_2O	NN; Phen	2	**16**
O	N; Bpy	H_2O	NN; Bpy	2	**17**

Scheme 5. Proposed strucutres of Cu^{II}-adducts.

(table 3), indicating that the perchlorate or the nitrate anions are situated outside the metal coordination sphere.

3.2. *IR spectra of the metal complexes*

IR spectra of the ligands and their metal complexes (table 2) are characterized mainly by the vibrational modes of the NH_2, OH(N, C=O, C=N and C=S groups). Comparison of the IR spectra of the metal complexes with those of the free ligands revealed that all complexes showed a broad band around 3500–3337 cm^{-1} assignable to νOH of the coordinated water molecules. The broad band around 2900 cm^{-1} is attributable to $\nu(OH\cdots N)$; intramolecular H-bonding of the phenolic group in the free ligands disappeared on complexation, indicating replacement of the phenolic proton by the metal ions and/or overlapping with ν(OH) of the coordinated water molecules. The two strong bands around 3400 and 3300 cm^{-1} assigned to ν_{as} and ν_s, respectively, of the $-NH_2$ group in the free ligands remained intact in all of the complexes, indicating the lack of participation of the $-NH_2$ group in chelation. The two strong bands at 1618 and 1623 cm^{-1} assigned to ν(C=N) for H_4L^1 and H_4L^2, respectively, were shifted to lower wavenumbers in all of the complexes, indicating the participation of the azomethine nitrogen in chelation.

The disappearance of the amide band-I and splitting of the ν(C=N) band into two bands at 1627–1617 and 1603–1586 cm^{-1} due to free and coordinated C=N groups, respectively, provides strong evidence that the enolic S/O participates in chelation after deprotonation leading to a covalent link.

In complex **5**, the chelating bidentate SO_4^{2-} group was indicated by the appearance of ν_3(S–O) bands at 1287 and 1087 cm^{-1}, which are characteristic for the high-symmetry T_d (tetrahedral) point group [15]. In addition, in complex **4**, the strong broad band

Table 3. Electronic spectra, magnetic moments and molar conductivity data for H_4L^1 and H_4L^2 and their metal complexes.

No.	Complex	Electronic spectral bands (nm)	μ_{eff}* (BM)	μ_{compl}[a] (BM)	Conductance[b] ($ohm^{-1}\,cm^2\,mol^{-1}$)
	H_4L^1	227, 249, 273, 297, 345	–	–	–
1	$[(L^1)Cu_2(H_2O)_2]\,½EtOH$	376, 421, 454, 484, 526, 541	1.65	2.24	36
2	$[(H_2L^1)Cu_2(OAc)_2(H_2O)_3]\,½EtOH$	384, 421, 563	1.60	2.0	25
3	$[(H_2L^1)_2Cu_3(H_2O)_2Cl_2]EtOH$	375, 390, 420, 453	1.57	2.47	49
4	$[(HL^1)Cu_2(H_2O)_7]ClO_4$	385, 421, 570	1.66	2.20	93
5	$[(H_2L^1)Cu_2(H_2O)_5SO_4]$	362, 388, 421, 436, 560	1.75	2.35	44
6	$[(HL^1)Cu_2(H_2O)_7]NO_3 \cdot ½EtOH$	362, 387, 421, 570	1.79	2.48	117
7	$[(H_2L^1)Cu_2(H_2O)_4(NO_3)_2]\,½EtOH$	362, 392, 423, 560	1.60	2.07	41
8	$[(H_2L^1)Cu_2Cl_2(H_2O)_4]EtOH$	382, 421, 548	1.60	2.15	31
9	$[(H_4L^1)Cu_2I_2(H_2O)_6]1\,½H_2O$	424, 445	Diamagnetic	Diamagnetic	42
10	$[(H_2L^1)Cu_2(Ox)(H_2O)_5]NO_3 \cdot ½EtOH$	356, 386, 423, 477	1.64	2.13	75
11	$[(H_2L^1)Cu_2(Phen)(NO_3)(H_2O)_4]NO_3 \cdot 2H_2O$	354, 388, 422, 452, 482, 518, 540	1.72	2.27	80
12	$[(H_2L^1)Cu_2(Bpy)(NO_3)(H_2O)_4]NO_3 \cdot EtOH$	54, 376, 422, 453, 487, 523, 744	1.79	2.36	75
13	$[(H_2L^1)_2Cu_2(H_2O)_2]EtOH$	424, 439, 550	1.76	2.31	20
	H_4L^2	225, 249, 273, 300, 333	–	–	–
14	$[(HL^2)Cu_2(H_2O)_2]NO_3 \cdot H_2O$	394, 678	1.61	2.18	102
15	$[(HL^2)Cu_2(H_2O)_2]NO_3 \cdot ¼EtOH$	389, 670	1.71	2.32	100
16	$[(H_2L^2)Cu_2(Phen)_2(H_2O)_3](NO_3)_2$	390, 540	1.90	2.55	146
17	$[(H_2L^2)Cu_2(Bpy)_2(H_2O)_3](NO_3)_2 \cdot H_2O$	383, 619	1.90	2.51	156
18	$[(H_3L^2)_2Cu_2(H_2O)_4]NO_3 \cdot 2\,½EtOH$	389, 728	1.76	2.30	192

*μ_{eff} is the magnetic moment of one cationic species in the complex.

[a] μ_{compl} is the total magnetic moments of all cations in the complex.

[b] Solution in DMF $(10^{-3\,mol}\,dm^{-3})$.

around 1080 cm^{-1} assigned to ν_3(Cl–O) indicates the noncoordinated (ionic) nature of the ClO_4^- ion [16] (T_d symmetry), consistent with conductance data for the complex. In complex **2**, the chelating bidentate CH_3COO^- group was supported by bands located at 1470 and 1412 cm^{-1} (absent in the spectra of H_4L^1). These two bands are due to $\nu_{as}(COO^-)$ and $\nu_s(COO^-)$, respectively. The separation of the two bands, $\Delta\nu = (\nu_{as} - \nu_s) = 58$ cm^{-1}, is comparable to the values cited for the bidentate character of the AcO^- group [17]; $\Delta\nu = 75$–80 cm^{-1}. On the other hand, the appearance of two new bands around 1440 (ν_5) and 1360 cm^{-1} (ν_1) in complex **7** confirmed the monodentate nature of the coordinated NO_3^- group (C_{2v} symmetry) [18]. As expected for C_{2v} symmetry, these two NO stretching bands are assigned to $\nu_{as}(NO_2)$ and $\nu_s(NO_2)$, respectively. In the electrolytic complexes **4**, **6**, **10–12** and **14–18**, the NO_3^- anion showed a new band around 1431–1390 cm^{-1} confirming its ionic nature [19]. For the mixed ligand complexes **10–12**, **16** and **17**, new bands around 1492–1477 cm^{-1} attributed to the coordinated C=N of the heterocyclic aromatic base (Phen, Bpy or oxine) indicate N-coordination [20,21]. Finally, for the dimeric complexes **13** and **18**, no band assignment is available [15]. Support for the above interpretation is the appearance of the nonligand bands at 560–400 [ν(M–O)], 400–320 [ν(M–N)] and 320–260 cm^{-1} [ν(M–S)].

3.3. *Electronic and ESR spectroscopy and magnetic moment measurements*

Visible spectra of the metal complexes (table 3) were recorded in DMF solutions. Comparison of the spectra of the free ligands and their complexes showed the persistence of the ligand bands in all complexes. The bands of the free ligands were shifted slightly in all of the complexes. New bands were also observed in the visible region due to d–d transitions (table 3). CT transitions are usually of higher energy than d–d transitions, thus they usually lie at the extreme blue end of the visible spectrum or in the ultraviolet (UV) region. Hence, the very intense bands displayed by the complexes at lower wavelengths (higher energy absorptions) are most likely due to ligand-to-Cu^{II} CT transitions, commonly of the (ligand) p to d (metal) [22]. Because of the Jahn–Teller distortion and the low symmetry of the environment around Cu^{II} (d^9), detailed interpretations of the spectra and magnetic properties are somewhat complicated [23]. Almost all of the complexes are blue or green due to the presence of an absorption band around 540–728 nm (table 3). Exceptions are generally caused by CT bands (strong UV bands tailing off into the blue end of the visible spectrum), thus causing the color to appear red or brown [23]. The magnetic moments of Cu^{II} complexes (table 3) lie in the range 1.57–1.90 BM/Cu^{II} ion, which is consistent with one unpaired electron (d^9).

Different geometries for square planar (**1**, **14**, **15**), square pyramidal (**13**) and distorted octahedral (the rest) structures are indicated by their visible and ESR spectra. The square planar complexes **1** and **14** are well defined from their ESR spectra, showing broad signals with $g_{eff} = 1.771$ and 1.915, respectively. The visible spectra (table 3) of the Cu^{II} complexes are more or less similar but indicate distorted octahedral geometry around the Cu^{II} ions. The bands and/or shoulders around 540–728 nm (table 3) are consistent with tetragonally distorted octahedra [23]. The higher energy bands may be due to CT transitions from ligands to Cu^{II} ions. The ESR spectrum of $[(H_2L^1)Cu_2(H_2O)_5SO_4]$ (**5**), as a typical example, shows a broad signal at g-value 1.859 and a shoulder at g-value 1.748. The former band would be assigned to $g_{||}$ and the latter shoulder to $g_{\perp}$. These results indicate a distorted octahedra. The broadening of the ESR signals would be due to the interaction between Cu^{II} ions present in nonequivalent lattice positions.

The difference between the coordinating sites of both H_4L^1 (SNO) and H_4L^2 (ONO) is reflected in the visible and ESR spectra as well as by the magnetic moments of their complexes (table 3) as follows. (i) A shift to higher energy (blue shift) was observed for S-bonded compared to O-bonded complexes. (ii) A decrease in μ_{eff} values was observed for S-bonded Cu^{II} complexes (1.57–1.79 BM) compared to O-bonded Cu^{II} complexes (1.60–1.90 BM), indicating a stronger interaction for S-bonded compared to O-bonded complexes. (iii) A decrease of 0.144 in g_{eff} values was observed for the S-bonded complex (**1**) compared to the O-bonded complex (**14**), revealing that the ESR parameters are dependent on the coordinating atoms. This type of behavior has been observed for Schiff-base complexes [24,25] and is attributed to (a) higher covalency of Cu–S compared to Cu–O bonds and (b) higher spin–orbit coupling constants for S than for O. Both factors reduce the spin–orbit contribution of the Cu^{II} ion to the *g*-tensor, decreasing the *g*-values [26].

3.4. *Mass spectra of the metal complexes*

Mass spectra of the complexes provide good evidence for their molecular formulae: $[(HL^1)Cu_2(H_2O)_7]ClO_4$ (**4**, FW 690.05), $[(H_2L^1)_2Cu_2(H_2O)_5SO_4]$ (**5**, FW 651.64), $[(H_2L^1)_2Cu_2(H_2O)_2]EtOH$ (**13**, FW 886.02) and $[(HL^2)Cu_2(H_2O)_2]NO_3 \cdot H_2O$ (**14**, FW 548.42) were selected as representative complexes. The mass spectra of these complexes showed peaks at *m*/*e* 687, 649, 842 and 533, which agree with the formula weights of the nonhydrated or solvated complexes $[(HL^1)Cu_2(H_2O)_7]ClO_4$ (FW 690), $[(H_2L^1)_2Cu_2(H_2O)_5SO_4]$ (FW 651.64), $[(H_2L^1)_2Cu_2(H_2O)_2]$ (FW 840) and $[(HL^2)Cu_2(H_2O)_2]NO_3$ (FW 530.42), respectively. On the other hand, the mass spectrum of the trinuclear complex $[(H_2L^1)_2Cu_3(H_2O)_2Cl_2]EtOH$ (**3**, FW 1020.47) showed the molecular ion peak at 1020.3, confirming its formula weight.

3.5. *Thermal analyses (TG-DSC)*

The aim of our thermal analyses was to obtain information concerning the thermal stability of the chelates investigated and to decide whether water or ethanol molecules are in the inner or outer coordination sphere of the metal ion. The thermograms of the chelates can be subdivided into two or three main regions depending on the nature of the chelates. (i) The first region extends up to 142°C corresponding to the weight loss of the hydrated water molecules and/or solvated ethanol molecules during one exothermic process. (ii) The second region extends up to 288°C corresponding to the weight loss of the coordinated water molecules to verify the transformations of octahedral or square pyramidal complexes to a square planar complex in most systems during a strongly endothermic process. (iii) Above 288°C, the complexes begin to decompose, at first slowly, then more rapidly up to 800°C with the formation of Cu_2O. The metal content was found to be concordant with the results of the elemental analyses. However, these general features depend on the nature of each complex.

3.6. *Antibacterial and antifungal activity*

H_4L^1 and its metal complexes were screened for both antifungal and antibacterial activity (table 4). The bacteria used were *Rhizobium* and the fungus was

Fusarium-Oxysporium. Inspection of the data given in table 4 reveals that: (i) all of the metal complexes of H_4L^1 show enhanced activity towards *Rhizobium* compared with the ligand itself, while the activity towards *Fusarium-Oxysporium* decreases upon complexation, and (ii) the anions play a significant role in antibacterial activity. When Cu^{II} chelates having different anions were screened, the degree of bactericidal activity varied greatly in the order: $NO_3^- > ClO_4^- > CH_3COO^- > Cl^- > SO_4^{2-}$.

Table 4. Antibacterial and antifungal activities of the H_4L^1 ligand and its complexes.

	Zone of inhibition (cm)	
Complex	*Rhizobium*	*Fusarium-Oxysporium*
H_4L^1	1.7	3.5
1	2.5	2.1
2	3.1	1.8
3	2.7	1.5
4	3.6	0.9
5	2.3	1.3
6	3.8	2.0
7	3.7	1.7
8	2.8	1.4
9	2.6	1.4
10	3.4	2.9
11	3.2	1.7
12	3.6	1.2
13	3.2	2.8

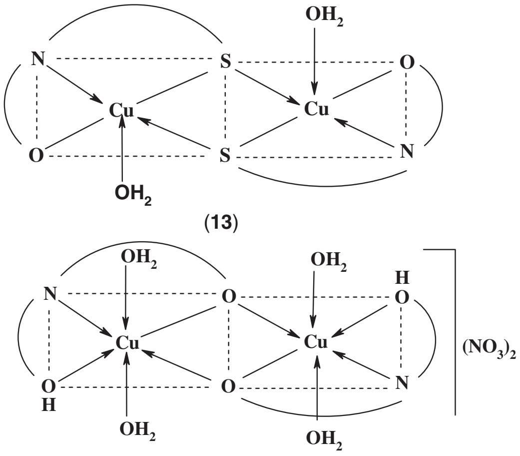

(**13**)

(**18**)

Scheme 6. Proposed structures of diameric Cu^{II} complexes.

4. Conclusions

As shown in schemes 3 and 5, both H_4L^1 and H_4L^2 ligands squeeze the SNONS and ONONO compartments to generate cavities of the right size to accommodate two Cu^{II} ions in different stereochemical configurations, Cu_2(SNONS) or Cu_2(ONONO) cores. By contrast, squeezing of the SNNS compartment by two H_4L^1 molecules might also generate cavities of the right size to accommodate three Cu^{II} ions via S-bridging (scheme 4; complex **3**). This is the only trinuclear complex in this investigation with a unique mode of bonding. Models showed that all the donor atoms (SNNS) are simultaneously accessible to the Cu^{II} ions. Another unique mode of bonding was observed for the diamagnetic Cu^I complex (scheme 4; complex **9**) in which H_4L^1 acts as a neutral tetradentate ligand (neutral bidentate NS/Cu^I ion). The reactivity of the S-bonded and O-bonded Cu^{II} complexes (**1** and **14**) towards the aromatic bases Phen and Bpy (NN-donors) afforded adducts having a molar ratio (Cu^{II} : ligand : base) 2 : 1 : 1 for the S-bonded and 2 : 1 : 2 for the O-bonded complexes (scheme 5; complexes **11**, **12**, **16**, **17**), reflecting the bulkiness of S compared to O. Surprisingly, both complexes **1** and **14** were found to be unreactive towards the aliphatic base Tmen (NN-donor) but formed dimeric complexes (scheme 6). This may be due to the presence of four bulky methyl groups attached directly to the coordinating sites of Tmen. The S-bonded complex **1** showed a higher reactivity towards oxine (NO-donor) and formed an adduct (scheme 5; complex **10**), while the O-bonded complex **14** did not (scheme 2; complex **15**).

In conclusion, the ligands behave as tetra-, tri-, di- or monobasic or neutral hexa-, penta-, tetra- or tridentates depending on the pH of the reaction medium, the experimental conditions and the metal ions and their counterions, as well as the presence of other ligands, such as Phen, Bpy, Tmen or oxine. Based on our results, the proposed structures of the complexes are given in schemes 2–6.

References

[1] E.W. Ainscough, A.M. Brodie, J.D. Ranford, J.M. Waters, *J. Chem. Soc., Dalton Trans.* 1251 (1997).
[2] P. Souza, A.I. Matesan, V. Fernandez, *J. Chem. Soc., Dalton Trans.* 3011 (1996).
[3] D.X. West, A.E. Liberta, S.B. Padhye, R.C. Chikate, P.B. Sonawane, A.S. Kumbhar, R.G. Yerande, *Coord. Chem. Rev.* **123**, 49 (1993).
[4] S. Padhye, G.B. Kauffman, *Coord. Chem. Rev.* **63**, 127 (1985).
[5] D.X. West, S.B. Padhye, P.B. Sonawane, *Struct. Bonding* **66**, 1 (1991).
[6] X. Li, Z. Sun, J.C. Chang, *Synth. React. Inorg. Met.-Org. Chem.* **18**, 657 (1988).
[7] M.F. Iskander, T.E. Khalil, R. Werner, W. Haase, I. Svoboda, H. Fuess, *Polyhedron* **19**, 1181 (2000).
[8] H. Nishioka, T. Kumagai, T. Nagahiro, *Microchem. J.* **50**, 88 (1994).
[9] Y. Tian, C. Duan, C. Zaho, X. You, *Inorg. Chem.* **36**, 1247 (1997).
[10] Y.D. Kulkarni, A. Rowhani, *J. Indian Chem. Soc.* **67**, 46 (1990).
[11] S.M.E. Khalil, H.S. Seleem, B.A. El-Shetary, M. Shebl, *J. Coord. Chem.* **55**, 883 (2002).
[12] H.S. Seleem, M. El-Behairy, M. Mashaly, H. Mena, *J. Serb. Chem. Soc.* **67**, 243 (2002).
[13] O.P. Pandey, *Polyhedron* **6**, 1021 (1987).
[14] C. He, C.Y. Duan, C.J. Fang, Y.J. Liu, Q.J. Meng, *J. Chem. Soc., Dalton Trans.* 1207 (2000).
[15] K. Nakamoto, *Infrared and Raman Spectra of Inorganic and Coordination Compounds*, 5th Edn, John Wiley and Sons, New York (1997).
[16] L.M. Fostiak, I. García, J.K. Swearingen, E. Bermejo, A. Castiñeiras, D.X. West, *Polyhedron* **22**, 83 (2003).
[17] J.K. Puri, V.K. Vats, A. Miglani, *Synth. React. Inorg. Met.-Org. Chem.* **31**, 1063 (2001).
[18] S.M.E. Khalil, K.A. Bashir, *J. Coord. Chem.* **55**, 681 (2002).
[19] Q. Han, F. Jian, L. Lu, X. Wang, *J. Coord. Chem.* **55**, 633 (2002).
[20] C. Yan, Y. Li, *Synth. React. Inorg. Met.-Org. Chem.* **30**, 99 (2000).
[21] Y. Tang, X. Gan, M. Ton, X. Zheng, *Polyhedron* **17**, 429 (1998).
[22] B.S. Garg, D.N. Kumar, *Spectrochim. Acta* **59**, 229 (2003).
[23] F.A. Cotton, G. Wilkinson, *Advanced Inorganic Chemistry*, 4th Edn, John Wiley and Sons, New York (1980).
[24] E. Pereira, L. Gomes, B. Castro, *J. Chem. Soc., Dalton Trans.* 629 (1998).
[25] E. Pereira, L. Gomes, B. Castro, *Inorg. Chim. Acta* **271**, 83 (1998).
[26] L. Gomes, E. Pereira, B. Castro, *J. Chem. Soc., Dalton Trans.* 629 (1998).